Subdiffusion and the cage effect studied near the colloidal glass transition

Eric R. Weeks [a,*], D. A. Weitz [b]

[a] *Physics Department, Emory University, Atlanta, GA 30322, USA*

[b] *DEAS and Physics Department, Harvard University, Cambridge, MA 02138, USA*

Abstract

The dynamics of a glass-forming material slow greatly near the glass transition, and molecular motion becomes inhibited. We use confocal microscopy to investigate the motion of colloidal particles near the colloidal glass transition. As the concentration in a dense colloidal suspension is increased, particles become confined in transient cages formed by their neighbors. This prevents them from diffusing freely throughout the sample. We quantify the properties of these cages by measuring temporal anticorrelations of the particles' displacements. The local cage properties are related to the subdiffusive rise of the mean square displacement: over a broad range of time scales, the mean square displacement grows slower than linearly in time.

Key words: Glass transition, colloids, anomalous diffusion, cage effect
PACS: 61.43.Fs, 64.70.Pf, 82.70.Dd, 05.40.Fb

1 Introduction

As glass-forming materials are cooled, the sharply increasing viscosity of the liquid is accompanied by equally dramatic changes in the motion of tracer particles within the material [1]. In particular, the mean square displacement $\langle \Delta x^2 \rangle$ (MSD) of an ensemble of tracer particles embedded in a glass-forming material forms a plateau at intermediate lag times, reflecting the crowding of the particles which prevents easy rearrangements [see Fig. 1(a)]. At longer lag times, the MSD shows an upturn, returning to diffusive motion, albeit with

* Corresponding author.
Email address: weeks@physics.emory.edu (Eric R. Weeks).

a greatly reduced diffusion coefficient ($\langle \Delta x^2 \rangle \sim 2D_\infty \Delta t$). Dense colloidal suspensions are simple materials which undergo a glass transition as the particle concentration increases, and provide a way to directly study the anomalous kinetics of the colloidal particles near the glass transition, to determine how the local motion of individual particles gives rise to the unusual behavior of the ensemble MSD [2,3]. The plateau in the MSD is subdiffusive: for a range of time scales Δt, $\langle \Delta x^2 \rangle$ grows as $\langle \Delta x^2 \rangle \sim (\Delta t)^\gamma$ with $\gamma < 1$; $\gamma = 1$ is the more typical diffusive case. Typically subdiffusion arises when a system possesses memory [4]. In this work, we test this by looking for temporal correlations in the particle motions. We find that these correlations do exist and are due to the "cage effect" of glassy systems (see Fig. 2). We characterize this cage effect, and directly connect the local description of particle caging to the subdiffusive plateau in the MSD and the lag-time dependent anomalous diffusion exponent $\gamma(\Delta t)$.

2 Experimental procedure

Our samples are colloidal poly-(methylmethacrylate) (PMMA) particles, sterically stabilized by a thin layer of poly-12-hydroxystearic acid [2,5,6]. They are in an organic solvent mixture of cyclohexylbromide and decalin, chosen to closely match the density and index of refraction of the particles [5]. The particles have a radius $a = 1.18$ μm and a polydispersity of $\sim$5%. They are dyed with rhodamine dye, which results in a slight charging of the particles. Despite this slight charge, their phase behavior is similar to colloidal hard spheres [7]: we find $\phi_{\rm freeze} = 0.38$ and $\phi_{\rm melt} = 0.42$ (for hard spheres these values are $\phi_f = 0.494$ and $\phi_m = 0.545$). As the concentration is further increased, we see a glass transition at $\phi_{\rm g} \approx 0.58$, in agreement with what is seen for hard spheres. Samples with $\phi > \phi_g$ do not form crystals in the bulk even after they have been sitting for several months. Moreover, the diffusion constant for such samples goes to zero – the samples become nonergodic [1].

We view the colloidal particles with a fast scanning laser confocal microscope, to obtain three-dimensional images from deep within the sample [2,3,5,8]. In practice, we focus at least 30 μm from the coverslip of the sample chamber, to avoid wall effects. By taking a series of three-dimensional images at intervals of 10-20 s, we are able to follow the motion of several thousand colloidal particles for several hours. We identify particle centers with an accuracy of 0.03 μm horizontally and 0.05 μm vertically; the poorer vertical resolution is due to optical limitations of the microscope. For further details, see Refs. [5,9].

3 Results

We calculate the mean square displacement $\langle \Delta x^2 \rangle$ from the measured particle positions, and several typical curves are shown in Fig. 1(a). The data at short Δt (less than 10 s) is obtained from two-dimensional measurements within the three dimensional sample, in order to improve the time resolution. At the shortest lag times, $\langle \Delta x^2 \rangle$ increases due to the diffusive motion of the particles. At intermediate time scales, the MSD has a plateau, which becomes more pronounced as the volume fraction ϕ increases toward $\phi_g \approx 0.58$. This plateau is due to the cage effect: particles are trapped in transient cages formed by their neighbors, and thus cannot diffuse freely through the sample [1,10]. At the largest Δt, the cages rearrange, and particles are able to diffuse throughout the sample, albeit with a greatly decreased diffusion coefficient D_∞ [10–12]. This can be seen in the particle trajectories shown in Fig. 2. Figure 2(a) shows two-dimensional projections of trajectories of several particles within a small region. The two particles marked *b* and *c* are magnified to the right, and show the difference between caged motion, and the rearrangements.

The cage rearrangements – that is, the relatively rapid shifts in particle positions seen in Fig. 2 – are reflected in broad tails for the distribution of particle displacements [12–15]. These distributions are shown by the symbols in Fig. 3(a). The time scales for the displacements are chosen to be comparable to the end of the MSD plateau. The majority of particles move only short distances, as they are confined within cages. However, the distributions show that a nontrivial fraction of particles do move large distances, more than would be expected if the distributions of displacements were gaussian [dotted lines in Fig. 3(a)]. A traditional way to quantify the relative size of the tails of the distribution is to calculate a nongaussian parameter, which compares the fourth moment of the distribution to the second moment:

$$\alpha_2(\Delta t) = \frac{3\langle \Delta r^4(\Delta t) \rangle}{5\langle \Delta r^2(\Delta t) \rangle^2} - 1 \tag{1}$$

which is zero for a gaussian distribution, and larger when the distribution is broader (for example, $\alpha_2 = 1$ for an exponential distribution) [12,15–17]. This parameter is close to zero at small and large lag times Δt, and is a maximum at an intermediate value Δt^* which we use to define the cage rearrangement time scale [11,12]. This time scale is indicated by vertical bars in Fig. 1(a), and corresponds qualitatively with the end of the MSD plateau.

To quantify the cage effect, we wish to look for temporal correlations in a particle's motion; we follow the method of Doliwa and Heuer [10,11]. In particular, if a particle moves in one direction for a period of time, its neighboring particles (the "cage") will prevent further motion in that direction, and may

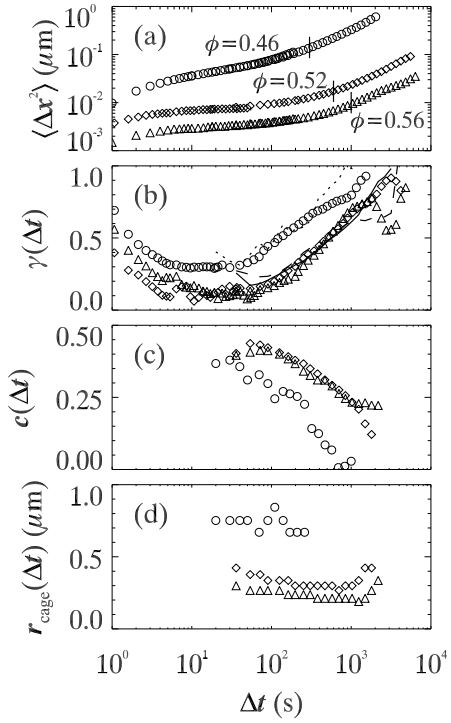

Fig. 1. (a) Mean square displacement for three "supercooled fluids," with volume fractions ϕ as indicated. The vertical lines indicate the cage rearrangement time scale Δt^*. (b) The symbols indicate the measured anomalous diffusion exponent $\gamma(\Delta t)$, equivalent to the logarithmic slope of $\langle \Delta x^2 \rangle$. The lines show the predicted value $\gamma_{\rm est}$ based on Eq. 3 (dotted line $\phi = 0.46$, solid line $\phi = 0.52$, and dashed line $\phi = 0.56$). (c) The anticorrelation scale factor $c(\Delta t)$ from Eq. 2; see text for details. (d) $r_{\rm cage}$ as a function of Δt. The symbols in (b-d) are the same as part (a).

push the first particle back toward the middle of the cage. In this way, the positions of the neighboring particles, which have shifted slightly to allow the interior particle to move, provide a "memory" of the interior particle's motion. Thus we expect that usually a particle's motion will be temporally anticorrelated, unless it is involved in a cage rearrangement (and thus moves and then stays in its new position). To look for this, we pick a time scale Δt and then consider displacement vectors for each particle, $\Delta\vec{r}_{mn} = \vec{r}(n\Delta t) - \vec{r}(m\Delta t)$. In particular we wish to determine how $\Delta\vec{r}_{12}$ depends on $\Delta\vec{r}_{01}$, and how this depends on the time scale Δt [10].

Anticipating that $\Delta\vec{r}_{12}$ is directionally correlated with $\Delta\vec{r}_{01}$, we consider two components of $\Delta\vec{r}_{12}$: x_{12} is the component of $\Delta\vec{r}_{12}$ parallel to $\Delta\vec{r}_{01}$, the original displacement, and y_{12} is the component of $\Delta\vec{r}_{12}$ along an arbitrarily chosen direction perpendicular to $\vec{r}_{01}$ [10]. Because of the arbitrariness in calculating y_{12}, the average $\langle y_{12} \rangle = 0$. For dilute samples, caging does not occur and $\langle x_{12} \rangle = 0$; $\langle x_{12} \rangle$ will be negative if memory effects are present. Particles which initially move farther must move their neighbors farther as well, and so we expect that $\langle x_{12} \rangle$ will depend on how far a particle has originally moved,

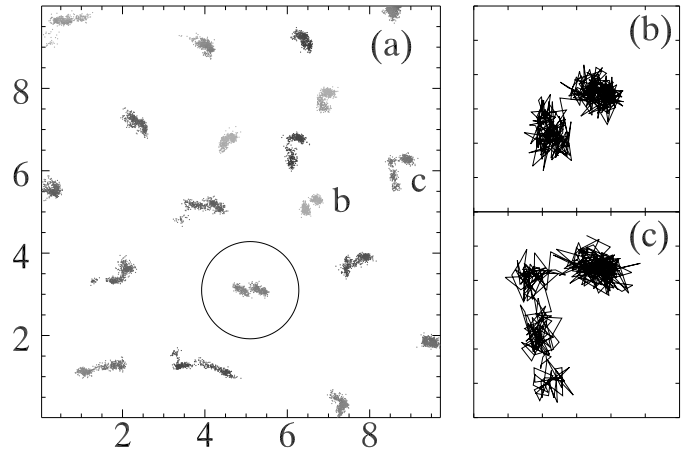

Fig. 2. (a) Trajectories of particles from a sample with $\phi = 0.52$, over a 2 hour period. The axes are labeled in microns, and the circle illustrates the particle size. These trajectories are from particles within a 2.5 μm thick region within the sample; the gray shades indicate vertical distance (darker is closer to the coverslip). (b) and (c) are magnifications of two of the trajectories, with tick marks indicating 0.2 μm spacings. These two particles alternate between being trapped in a local cage, and a slight jump to a new location when the cage rearranges.

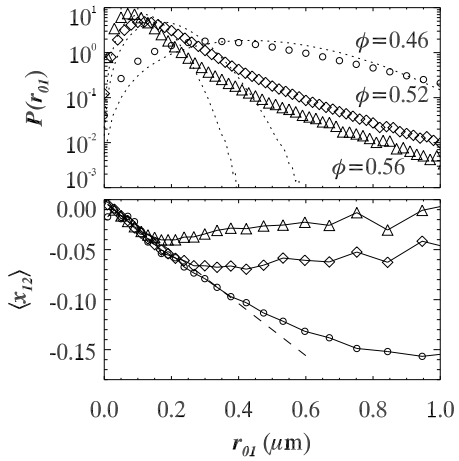

Fig. 3. (a) Probability distribution functions for displacements r_{01} with time scales $\Delta t = 260$ s for $\phi = 0.46$, 700 s for $\phi = 0.52$, and 1000 s for $\phi = 0.56$. (b) $\langle x_{12} \rangle$ as a function of r_{01} for the same data shown in (a). The values of Δt for the three data sets have been chosen to produce similar behavior at small r_{01}, which in these cases is reasonably well described as $\langle x_{12} \rangle = -(0.26) r_{01}$ (indicated by the dashed line). The departure from the small r_{01} behavior occurs at $r_{\rm cage} \approx 0.75, 0.35, 0.25$ μm for $\phi = 0.46, 0.52, 0.56$.

$r_{01} = |\vec{r}_{01}|$. To investigate this we compute the average value $\langle x_{12} \rangle$ as a function of r_{01}, and plot this in Fig. 3(b) for three different volume fractions [10]. Δt has been chosen so that the curves have similar behavior at small r_{01}, and also to be close to the cage rearrangement time scale Δt^*. The average is taken over all particles and all initial times. x_{12} is negative, indicating anticorrelated

motion: particles which move in one direction during the first time interval will, on average, move in the opposite direction during the subsequent time interval. This is a direct signature of the cage effect. Moreover, for particles with small displacements r_{01}, the average subsequent displacement $\langle x_{12} \rangle$ is linearly proportional to r_{01}, as indicated by the dashed line in Fig. 3(b). For larger r_{01}, $\langle x_{12} \rangle$ is no longer proportional to r_{01}, and in fact becomes almost independent of r_{01} [10].

The departure from the linear behavior at small r_{01} occurs at smaller distances as the volume fraction ϕ increases toward the glass transition. The existence of two regimes – a linear response at small r_{01} and a breakdown of this linear response at larger r_{01} – suggests that the crossover point can be taken as $r_{\rm cage}$, and the two regimes be identified as caged particles and rearranging particles respectively. In other words, particles with $r_{01} < r_{\rm cage}$ typically remain caged, and the effect of the cage is to push the particle back toward its original position [10,11]. The strength of this effect is given by

$$\langle x_{12} \rangle = -c r_{01}, \tag{2}$$

with for example $c = 0.26$ for the data shown in Fig. 3(b). Particles with $r_{01} > r_{\rm cage}$ still tend to be pushed back, but not as far as predicted from linear extrapolation from the small r_{01} behavior: thus these particles may end up in new positions, and their behavior reflects cage rearrangements rather than caged motion. The changes seen in Fig. 3(b) as ϕ is increased shows that the cage size $r_{\rm cage}$ decreases as the glass transition is approached [18,19].

By studying the Δt dependence of the proportionality constant c and cage size $r_{\rm cage}$, we can better understand the MSD. The value of c depends strongly on the chosen time scale Δt, as shown in Fig. 1(c). In the middle of the MSD plateau, c is large, close to 0.5; at larger Δt it decreases, signaling a diminishing cage effect. $c(\Delta t)$ can be related to the logarithmic slope of the MSD [10], to directly connect the cage effect to the subdiffusive MSD plateau. Locally the MSD grows as $\langle \Delta r^2 \rangle \sim \Delta t^{\gamma(\Delta t)}$, with the anomalous diffusion exponent $\gamma(\Delta t)$ equal to the logarithmic derivative of $\langle \Delta x^2 \rangle$. This can be estimated as:

$$\begin{aligned}
\gamma_{\rm est}(\Delta t) &= \frac{d \ln \langle \Delta r^2 \rangle}{d \ln \Delta t} \\
&\approx \frac{\ln[|\Delta \vec{r}_{01} + \Delta \vec{r}_{12}|^2 / \langle r_{01}^2 \rangle]}{\ln(2\Delta t / \Delta t)} \\
&= \frac{\ln(2 + 2\langle x_{12} r_{01} \rangle / \langle r_{01}^2 \rangle)}{\ln 2} \\
&\approx 1 + \ln(1 - c(\Delta t))/\ln 2.
\end{aligned} \tag{3}$$

We have used $\langle r_{12}^2 \rangle = \langle r_{01}^2 \rangle$ (time invariance) and the final approximation uses

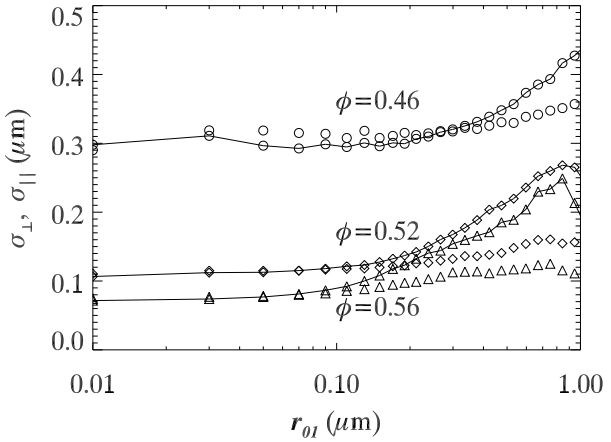

Fig. 4. $\sigma_\parallel$ (connected symbols) and $\sigma_\perp$ as a function of r_{01}, for three different volume fractions as indicated. The time scales are as in Fig. 3.

$\langle x_{12} r_{01} \rangle / \langle r_{01}^2 \rangle \approx \langle x_1 2 \rangle / \langle r_{01} \rangle \approx -c$, in analogy with Eq. 2; we have verified that these approximations are reasonable [11]. In Fig. 1(b) the symbols show $\gamma(\Delta t)$ computed directly from the MSD, and the lines show $\gamma_{\rm est}(\Delta t)$ calculated from Eq. 3. The subdiffusive plateau in the MSD is seen as a broad range of Δt for which $\gamma(\Delta t) < 1$, although it is also clear that γ does not have a constant value anywhere in the plateau, but rather is a smoothly evolving function of Δt. Moreover, the behavior of $\gamma(\Delta t)$ is well-captured by the calculated value based on $c(\Delta t)$, as shown by the agreement between the symbols (γ) and the lines ($\gamma_{\rm est}$). In other words, the subdiffusive behavior of the MSD is a direct consequence of the caged motion of the particles, as measured by Eq. 2. As Δt increases, the cage effect becomes less important, $c(\Delta t)$ decreases toward zero (no caging), and the MSD approaches diffusive behavior ($\gamma \to 1$).

The behavior of the cage size $r_{\rm cage}$ is shown in Fig. 1(d). $r_{\rm cage}$ is relatively insensitive to Δt, indicating the the size of the cage is more likely a static property [10,18]. The cage size decreases as the glass transition is approached, although it has a nonzero value at the glass transition [18,19]. The diffusive behavior of the MSD at large time scales can thus be thought of as due to the random walks of the individual particles, each taking steps of size $r_{\rm cage}$ in random directions [18]. On the cage rearrangement time scale Δt^*, only a few particles move (5 - 10 %) [2,12,18], and so in fact the average time between random walk steps is much larger than Δt^* as seen in Ref. [18].

Further insight into the cage effect can be found by studying the behavior of the total displacement $\Delta \vec{r}_{12}$ rather than focusing only on x_{12}, the component in the direction of $\Delta \vec{r}_{01}$. $\Delta \vec{r}_{12}$ can be decomposed into the deterministic part ($\langle x_{12} \rangle$ given by Eq. 2 and $\langle y_{12} \rangle = 0$), and a stochastic part. Both the deterministic and stochastic parts may may depend on r_{01}. To measure the importance of the stochastic part, we compute $\sigma_\parallel = \langle x_{12}^2 \rangle - \langle x_{12} \rangle^2$ and $\sigma_\perp = \langle y_{12}^2 \rangle - \langle y_{12} \rangle^2$, shown in Fig. 4 by the connected symbols and unconnected symbols, respec-

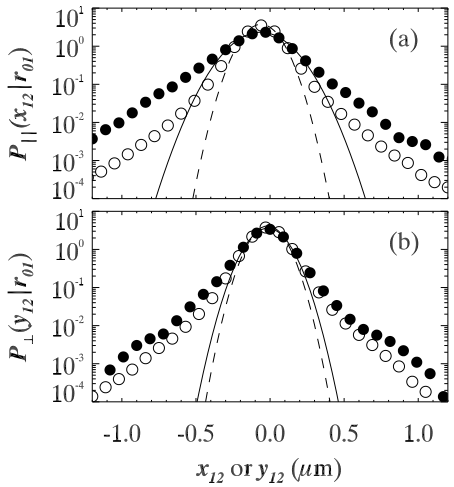

Fig. 5. (a) The functions $P_{\|}(x_{12}|r_{01};t)$ and (b) $P_{\perp}(y_{12}|r_{01};t)$, for $\phi = 0.52$ (a liquid), with $t = t^* = 600$ s. The open circles are all data for $r_{01} < r_{\rm cage} = 0.4$ μm and the closed circles are for $r_{01} > r_{\rm cage}$. The gaussian fits are shown as dashed lines for $r_{01} < r_{\rm cage}$ and solid lines for $r_{01} > r_{\rm cage}$, and have widths of $\sigma \approx 0.13$ μm for all except $\sigma_{\|}(r_{01} > r_{\rm cage} = 0.22$ μm. Similarly, the nongaussian parameter $\alpha_2 = 1.8$ for all except $P_{\|}(x_{12}|r_{01} > r_{\rm cage})$, which has $\alpha_2 = 1.0$.

tively. The behaviors of the parallel and perpendicular components are similar at small values of r_{01}, but differ markedly when the original displacement has a larger distance r_{01} [11]. The transverse component $\sigma_{\perp}$ is nearly constant as a function of r_{01}, but $\sigma_{\|}$ becomes much larger when r_{01} is larger. Again, any dependence whatsoever on r_{01} is indicative of memory in the system, and the increase in $\sigma_{\|}$ reflects a memory of *mobility*. Particles which move large distances originally (large values of r_{01}) are more mobile subsequently (large values of $\sigma_{\|}$), and in particular are more mobile along the direction of the original motion.

Confirmation of this is seen by plotting the distribution functions $P_{\|}(x_{12}|r_{01})$ and $P_{\perp}(y_{12}|r_{01})$ in Fig. 5, where the open circles are for $r_{01} < r_{\rm cage}$ and the closed circles are for $r_{01} > r_{\rm cage}$. Gaussian fits to these distribution functions are shown by the lines. All of the functions appear similar, except for $P_{\|}(x_{12};r_{01} > r_{\rm cage})$, which is significantly broader [solid circles in Fig. 5(a)]. Thus, particles which originally have larger displacements are more likely to continue moving in the same direction (large $x_{01} > 0$) or more likely to move a large distance backwards ($x_{01} < 0$), but slightly less likely to stay in the same position. Moreover, as $\sigma_{\|} \neq \sigma_{\perp}$, the particles undergoing cage rearrangements move in a highly anisotropic fashion. The distributions are broader than Gaussians, as can be seen by comparing the symbols to the lines; this is a reflection of the underlying broad distributions of the displacements, as shown in Fig. 3(a). Note also that the distributions shown in Fig. 5 are symmetric about the peak; this is unsurprising for $P_{\perp}(y_{12})$ and perhaps more surprising for $P_{\|}(x_{12})$.

4 Discussion

We have studied the microscopic motion of thousands of tracer particles in a concentrated colloidal sample, in order to understand the dramatic dynamical changes near the glass transition. In particular, near the glass transition, particles are confined to transient cages, resulting in temporal anticorrelations in particle displacements. We find that caging can be described as a deterministic anticorrelated motion, plus a stochastic part. The deterministic part is due to memory provided by the caging particles, which must adjust their positions to allow a particle to move, and subsequently push that particle back toward its original position. By quantifying these effects (as given by Eq. 2), we can connect the properties of the cage directly to the subdiffusive growth of the mean square displacement (MSD), shown in Fig. 1(a). The connection is quite good, as seen by comparing the lines and symbols in Fig. 1(b).

The long time behavior of the MSD is diffusive, as seen in Fig. 1(a). This can be thought of as due to the random walks taken by the individual particles, which alternate between being stuck in cages for a random duration, and a cage rearrangement motion of random length (see Fig. 2). A simple possibility which leads to diffusive motion at long times is that the cages responsible for the subdiffusive plateau have finite lifetimes with a characteristic time scale. An alternate possibility is that the cage rearrangement motions could be Lévy flights. Lévy flights are motions with an infinite mean square step size, in other words, cage rearrangements would involve movements that carry particles large distances. In such a way, diffusive motion at long times could be due to a competition between cages with infinite mean lifetime, and motions with infinite mean square lengths [4]. (These possibilities would suggest that the distribution for cage times and/or step sizes are power laws, for example $P(\Delta x) \sim (\Delta x)^{-\nu}$ for the cage rearrangement displacement Δx with $1 < \nu < 3$.) Lévy flights seem possible when looking at the broad tails shown in Fig. 3(a). However, at best Fig. 3(a) shows a truncated Lévy distribution. We do not see any particles making dramatic displacements much larger than their own radius; the trajectories shown in Fig. 2 making small adjustments are typical. It seems likelier that the characteristic step size is $r_{\rm cage}$, a small and finite distance, and thus the diffusive growth of the MSD as $\Delta t \to \infty$ is due to a finite cage lifetime [18]. In glassy samples, the cage rearrangements are no longer allowed, and thus the MSD will be subdiffusive at all times, and perhaps asymptotically reach a plateau; thus we expect these concepts to be even more useful in understanding the strange kinetics of nonergodic glassy samples.

We thank B. Doliwa and H. G. E. Hentschel for helpful discussions, and thank A. Schofield for providing our colloidal samples. This work was supported by NSF (DMR-9971432) and NASA (NAG3-2284).

References

[1] C. A. Angell, Science **267** (1995) 1924; F. H. Stillinger, Science **267** (1995) 1935; M. D. Ediger, C. A. Angell, S. R. Nagel, J. Phys. Chem. **100** (1996) 13200; C. A. Angell, J. Phys. Cond. Mat. **12** (2000) 6463.

[2] E. R. Weeks, J. C. Crocker, A. C. Levitt, A. Schofield, and D. A. Weitz, Science **287** (2000) 627.

[3] W. K. Kegel and A. van Blaaderen, Science **387** (2000) 290.

[4] E. R. Weeks and H. L. Swinney, Phys. Rev. E **57** (1998) 4915; J. P. Bouchaud and A. Georges, Phys. Rep. **195** (1990) 127.

[5] A. D. Dinsmore, E. R. Weeks, V. Prasad, A. C. Levitt, D. A. Weitz, App. Opt. **40** (2001) 4152.

[6] L. Antl et. al., Colloids and Surfaces **17** (1986) 67.

[7] P. N. Pusey and W. van Megen, Nature **320** (1986) 340.

[8] A. van Blaaderen and P. Wiltzius, Science **270** (1995) 1177.

[9] J. C. Crocker and D. G. Grier, J. Colloid Interface Sci. **179** (1996) 298.

[10] B. Doliwa and A. Heuer, Phys. Rev. Lett. **80** (1998) 4915.

[11] B. Doliwa and A. Heuer, J. Phys.: Condens. Matter **11** (1999) A277.

[12] W. Kob, C. Donati, S. J. Plimpton, P. H. Poole, S. C. Glotzer, Phys. Rev. Lett. **79** (1997) 2827; C. Donati et al., Phys. Rev. Lett. **80** (1998) 2338; C. Donati, S. C. Glotzer, P. H. Poole, Phys. Rev. Lett. **82** (1999) 5064.

[13] A. Kasper, E. Bartsch, H. Sillescu, Langmuir **14** (1998) 5004.

[14] A. H. Marcus, J. Schofield, S. A. Rice Phys. Rev. E **60** (1999) 5725.

[15] M. M. Hurley and P. Harrowell, J. Chem. Phys. **105** (1996) 10521.

[16] A. Rahman, Phys. Rev. **136** (1964) A405.

[17] W. Kob and H. C. Andersen, Phys. Rev. E **51** (1995) 4626.

[18] E. R. Weeks and D. A. Weitz, submitted to Phys. Rev. Lett. (2001) (cond-mat/0107279).

[19] P. Allegrini, J. F. Douglas, S. C. Glotzer, Phys. Rev. E **60** (1999) 5714.